

Structure-Activity Relationship of Hetarylpropylguanidines Aiming at the Development of Selective Histamine Receptor Ligands[†]

Steffen Pockes,* David Wifling, Armin Buschauer, and Sigurd Elz^[a]

This Paper is dedicated to the memory of Prof. Dr. Armin Buschauer (died on July 18, 2017).

New classes of alkylated hetarylpropylguanidines with different functionality and variation in spacer length were synthesized to determine their behavior at the four histamine receptor (H₁R, H₂R, H₃R, H₄R) subtypes. Alkylated guanidines with different terminal functional groups and varied basicity, like amine, guanidine and urea were developed, based on the lead structure SK&F 91486 (2). Furthermore, heteroatomic exchange at the guanidine structure of 2 led to simple analogues of the lead compound. Radioassays at all histamine receptor subtypes were accomplished, as well as organ bath studies at the guinea

pig (*gp*) ileum (*gp*H₁R) and right atrium (*gp*H₂R). Ligands with terminal functionalization led to, partially, highly affine and potent structures (two digit nanomolar), which showed up a bad selectivity profile within the histamine receptor family. While the benzoylurea derivative 144 demonstrated a preference towards the human (*h*) H₃R, *S*-methylisothiourea analogue 143 obtained high affinity at the *h*H₄R (pK_i=8.14) with moderate selectivity. The molecular basis of the latter finding was supported by computational studies.

Introduction

The biogenic amine histamine (1, Figure 1) is known to be the endogenous key modulator for histamine receptors in the human body.^[1] There it regulates a variety of effects via the four histamine receptor (HR) subtypes H₁, H₂, H₃ and H₄, each belonging to the superfamily of G-protein coupled receptors (GPCRs).^[2–6] The H₁R is expressed in several tissues (e.g., brain, blood vessels, gastrointestinal tract) and couples to a G_{q/11}-protein.^[7,8] For decades, H₁-antihistamines have been success-

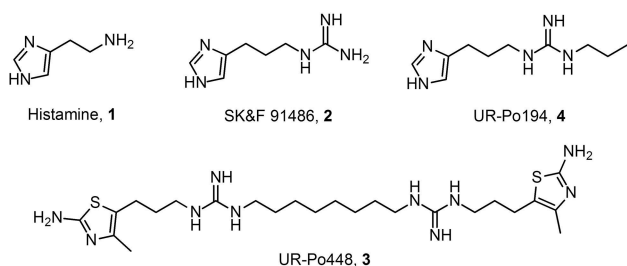


Figure 1. Structures of histamine and selected histamine receptor ligands (2–4).

[a] Dr. S. Pockes, Dr. D. Wifling, Prof. Dr. A. Buschauer, Prof. Dr. S. Elz
Institute of Pharmacy, Faculty of Chemistry and Pharmacy
University of Regensburg
Universitätsstraße 31, D-93053 Regensburg, Germany
E-mail: steffen.pockes@ur.de

Supporting information for this article is available on the WWW under
<https://doi.org/10.1002/open.201900011>

© 2019 The Authors. Published by Wiley-VCH Verlag GmbH & Co. KGaA.
This is an open access article under the terms of the Creative Commons
Attribution Non-Commercial NoDerivs License, which permits use and dis-
tribution in any medium, provided the original work is properly cited, the
use is non-commercial and no modifications or adaptations are made.

fully used for the treatment of allergic diseases as sedatives and antiemetics.^[9] The H₂R is mainly expressed in gastric parietal cells, in the heart, as well as in the brain and couples to a G_{α_s}-protein, which activates the adenylyl cyclase (AC).^[10,11] Prior to proton-pump inhibitors, such as omeprazole and pantoprazole,^[12] overstocking the market in the 1990s, H₂R antagonists like cimetidine have been one of the first blockbuster drugs for the treatment of gastroesophageal reflux disease (GERD) and peptic ulcer.^[13] The H₃R and H₄R are both coupled to G_{α_{v/o}}-proteins, but differentiate in their localization in the human body.^[14–16] While H₃R are widely expressed in the central nervous system,^[17] the H₄R is mainly found in immune and mast cells.^[5,15,18–20] Due to its function as an auto- and heteroreceptor in the brain, the H₃R is a promising potential target for various cognitive disorders, like Alzheimer's disease, Parkinson or Tourette syndrome.^[21–25] Even if the biological functions of the H₄R are not completely apparent, intensive research proved the involvement in allergic and inflammatory processes.^[26] For this reason, targeting the H₄R is expected to be crucial for the treatment of allergic rhinitis, rheumatoid arthritis or pruritus.^[27–30]

While the first antihistamines (H₁R), like mepyramine and diphenhydramine, as well as their functional behavior on guinea-pig organs were published in the 1930s, 1940s and 1950s,^[31–33] a large number of highly potent H₂R agonists like impromidine and arpromidine were released in the 1970s and 1980s.^[34–36] Deriving from the lead structure SK&F 91486 (2, Figure 1)^[37], a long-known ligand addressing histamine receptors, several classes of newly synthesized monomers were characterized in this study. A couple of previous projects, focusing on the development of potent H₂R agonists, observed an overlap of H₃R- and H₄R-related effects of imidazole-containing compounds.^[38] Heterocyclic replacement by amino

(methyl)thiazole, following amthamine,^[39] led to highly selective dimeric H₂R agonists, like UR–Po448 (**3**, Figure 1)^[40] and associated molecules.^[41–43] In addition, a switch away from imidazole-bearing compounds is recommended as these structures show poor pharmacokinetic properties due to interactions with cytochrome P450.^[44] Structural modifications around the guanidine group gave cyano-, carbamoyl-, acylguanidines and related structures, which showed up selectivity towards the H₃R or H₄R, respectively.^[45,46] In this project, we aimed to attaining insights into structure-activity relationships of novel ligands from the hetarylpropylguanidine-type. We wanted to close the gap between the monomeric lead structure **2**, the highly affine hH₄R ligand UR–Po194 (**4**, Figure 1)^[40] and the dimeric ligands described in the literature, e.g. **3**.^[40] Therefore, we created alkylated guanidines with various terminal functional groups of different basicity, like amine, guanidine, urea, including variable spacer length. Moreover, we synthesized a class of molecules focusing on the heteroatomic exchange at the guanidine moiety of **2** only to attain (thio)ureas and S-methylisothioreas. The final compounds were pharmacologically characterized with radioligand binding assays and the GTPγS binding assay to get binding as well as functional data. In addition, we analyzed all compounds by organ pharmacological studies on the guinea pig ileum and right atrium in order to receive information about their functional behavior under physiological conditions (*gp*H₁R (ileum), *gp*H₂R (right atrium)).

Results and Discussion

Chemistry

Syntheses of the amines **5–7** (Figure 2), which were used for the development of the final compounds were carried out according to the literature.^[39,41,47,48] The required precursors **17–27** for the terminal amines and guanidines were prepared according to previously reported procedures (Scheme 1) and adaptations.^[41,49,50] The isothiurea **10** proved to be a suitable guanidinylation reagent for the preparation of **23–27** and was obtained in a two-step synthesis by S-methylation of **8** and di-Boc-protection of **9** with two equivalents of Boc₂O (Scheme 1).^[41,51] Mono-Boc-protection of the respective diamines **11–16** was also carried out with Boc₂O to get **17–22** (Scheme 1). Due to the possibility of a di-protection a molar ratio of at least 1:5 (Boc₂O:diamine) was required in order to achieve yields >90%.^[49] The aforementioned di-Boc-protected guanidines **23–27** were prepared by dropping the guanidinylation reagent **10** into a solution of the appropriate diamine (**12–16**, 3 equiv) in DCM (Scheme 1).^[50]

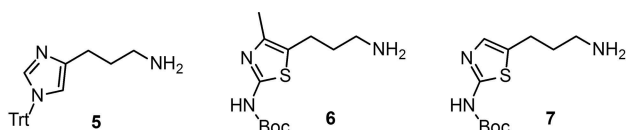
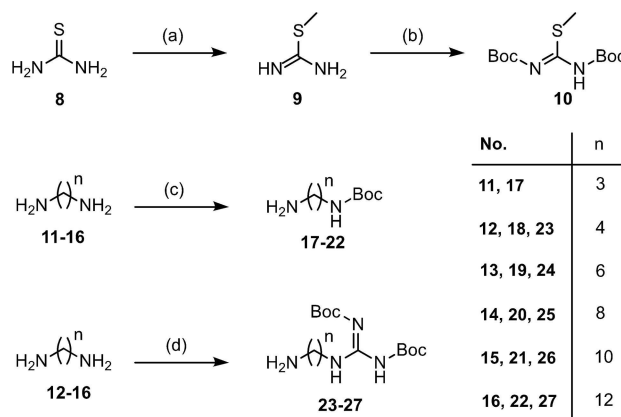


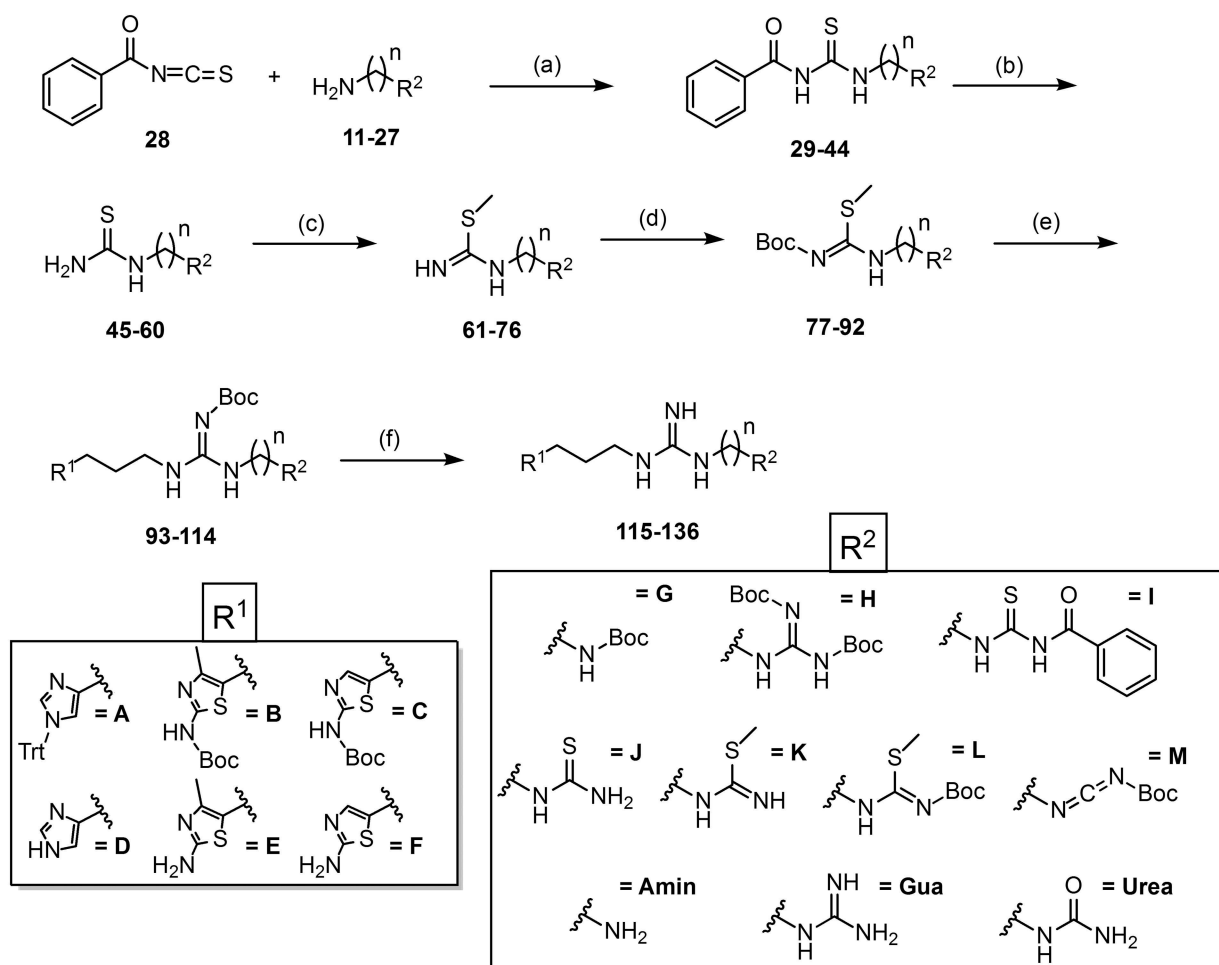
Figure 2. Structures of the amines **5–7**, which were used for the preparation of the final compounds **115–136** and **141–145** (cf. Scheme 1–3).



Scheme 1. Synthesis of the precursors **17–27**. Reagents and conditions: (a) CH₃I (1.1 equiv), MeCN, 1 h, reflux; (b) NEt₃ (1 equiv), Boc₂O (2 equiv), overnight, room temperature (rt); (c) diamine (5 equiv), Boc₂O (1 equiv), DCM, 2 h, 0 °C → rt; (d) diamine (3 equiv), **10** (1 equiv), DCM, overnight, rt.

The synthetic route for the preparation of **115–136** and **141–145** was adapted as previously described in the literature (Scheme 2 and 3).^[40,49,50,52–56] In a first step the relevant amine **11–27** attacks benzoyl isothiocyanate (**28**) via nucleophilic substitution to give benzoylthioureas **29–44** (Scheme 2).^[40,52] After alkaline hydrolysis yielding the corresponding thioureas **45–60**, the intermediates were treated with methyl iodide to receive **61–76** (Scheme 2).^[40,52] Prior to guanidinylation, the S-methylisothioureas were Boc-protected obtaining **77–92** (Scheme 2).^[40] Aminolysis of the guanidinylation reagents **77–92** with some of the amines **5–7** in presence of HgCl₂ and triethylamine gave **93–114** (Scheme 2).^[40,57] For the synthesis of the Boc-protected amines (**93–100**) and guanidines (**101–109**) one equivalent of HgCl₂ was used, while four equivalents of HgCl₂ were used for the preparation of the Boc-protected carbodiimides (**110–114**). The carbodiimides, which were converted into ureas in the next step, were unscheduled. It was planned to create the relative dimers, which were published by Pockes et al.^[40] The original synthetic description for one-site coupling was described with two equivalents of mercury chloride.^[41] This excess should be maintained for this two-site coupling. Contrary to our expectations the excess of HgCl₂ (4 equiv) – which facilitates the elimination of the S-methyl group by coordination to sulfur – led to mono-Boc-carbodiimides, where just one aminolysis was successful. This fact could be proven by NMR spectroscopy and mass spectrometry and a similar issue was already reported by Kim et al. in 1993.^[57] Afterwards, the use of HgCl₂ for one-site coupling was adjusted as described in 4.2.9, as well as for two-site coupling (cf. Pockes et al.)^[40]. In a last step the precursors were Boc-deprotected using trifluoroacetic acid (TFA) to get **115–136** as final compounds (Scheme 2).^[40]

The synthetic strategy for the final compounds **141–145** is depicted in Scheme 3. The same pattern was used for the nucleophilic addition to get **137** or **139** using **28** or benzoyl isocyanate (**138**) together with the amine **5** (Scheme 3).^[40,52] **137** was further processed in two different ways, getting **140** by alkaline hydrolysis and **141** by deprotection under acidic



Compounds 29-92:

R ² \ n	3	4	6	8	10	12
G	29,45 61,77	30,46 62,78	31,47 63,79	32,48 64,80	33,49 65,81	34,50 66,82
H	-	35,51 67,83	36,52 68,84	37,53 69,85	38,54 70,86	39,55 71,87
I	40	41	42	43	44	-
J	56	57	58	59	60	-
K	72	73	74	75	76	-
L	88	89	90	91	92	-

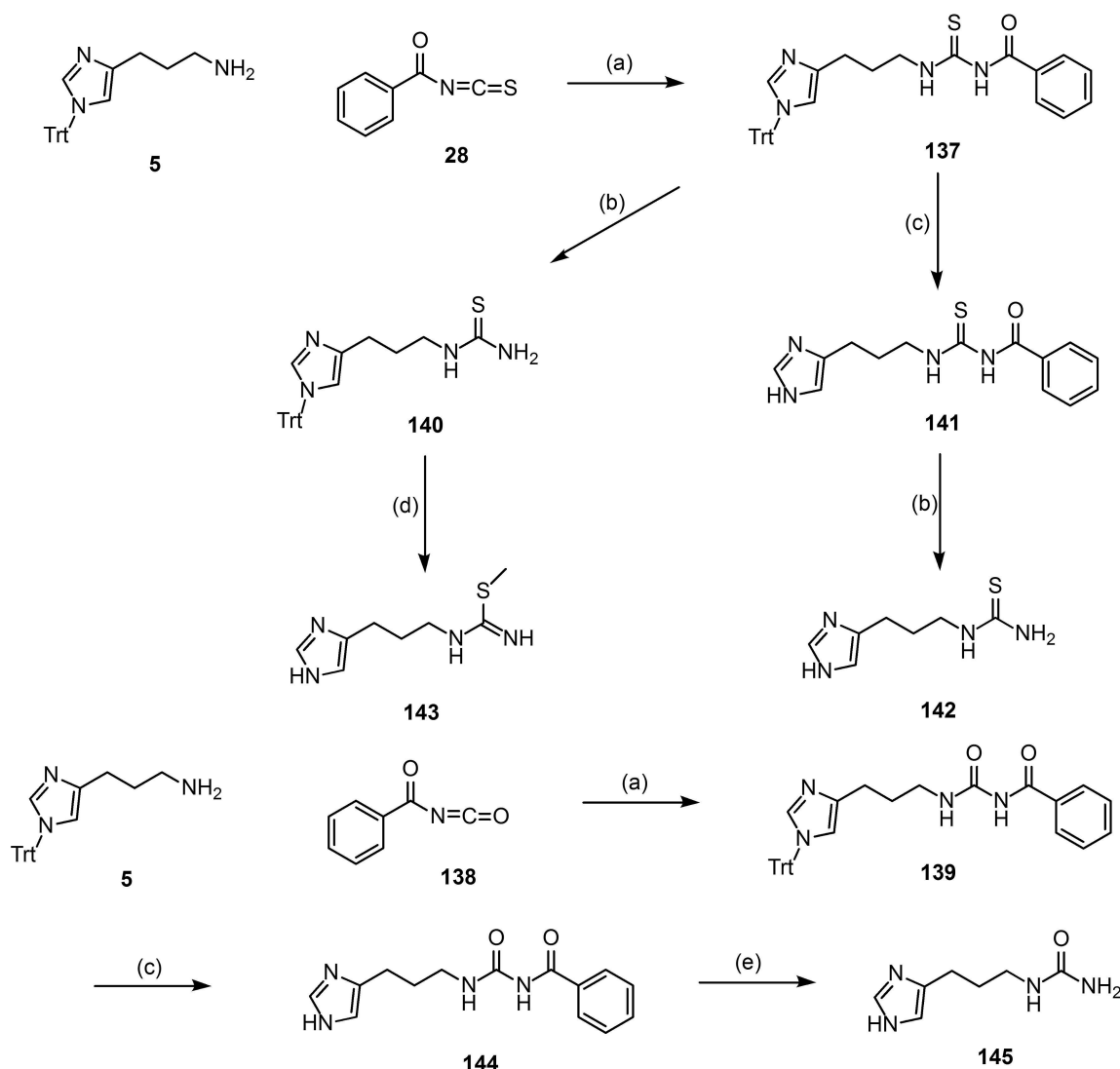
Compounds 93-136:

No.	R ¹	R ²	n	No.	R ¹	R ²	n
93/115	A/D	G/Amin	3	104/126	A/D	H/Gua	10
94/116	A/D	G/Amin	4	105/127	A/D	H/Gua	12
95/117	A/D	G/Amin	6	106/128	B/E	H/Gua	8
96/118	A/D	G/Amin	8	107/129	C/F	H/Gua	8
97/119	A/D	G/Amin	10	108/130	B/E	H/Gua	12
98/120	A/D	G/Amin	12	109/131	C/F	H/Gua	12
99/121	B/E	G/Amin	12	110/132	A/D	M/Urea	3
100/122	C/F	G/Amin	12	111/133	A/D	M/Urea	4
101/123	A/D	H/Gua	4	112/134	A/D	M/Urea	6
102/124	A/D	H/Gua	6	113/135	A/D	M/Urea	8
103/125	A/D	H/Gua	8	114/136	A/D	M/Urea	10

Scheme 2. Synthesis of the HR ligands 115–136. Reagents and conditions: (a) amine/diamine (1 equiv), **28** (1 equiv/2 equiv), DCM, 2 h/overnight, 0 °C → rt; (b) K₂CO₃ (2.1 equiv/4.1 equiv), MeOH/H₂O (7/3, v/v), 3–5 h, rt; (c) CH₃I (1.1 equiv/2.1 equiv), MeCN, 1 h, reflux; (d) NEt₃ (1 equiv/2 equiv), Boc₂O (1 equiv/2 equiv), overnight, rt; (e) **5**, **6** or **7** (1 equiv/2 equiv), HgCl₂ (1 equiv/4 equiv), NEt₃ (3 equiv/6 equiv), DCM, overnight, rt; (f) 20% TFA, DCM, overnight, reflux.

conditions (Scheme 3).^[40,52] Moreover, the benzoyl isothiocyanate **141** was hydrolysed with potassium carbonate to give the thiourea **142** (Scheme 3).^[40,52] To complete the second route, **140** was first deprotected with hydrogen iodide (66%) and directly handled with methyl iodide yielding **143** (Scheme 3).^[53,54] To create the urea analogues, the trityl group

of **139** was first cleaved with TFA to get the final compound **144**,^[40] followed by alkaline hydrolysis with sodium hydroxide solution (1 M) under reflux obtaining **145** (Scheme 3).^[56] Usual basic hydrolysis with potassium carbonate was not successful in this case, not even after several hours of reflux. Compounds **141**^[53], **142**^[53] and **143**^[54,35] were already described in the



Scheme 3. Synthesis of the SK&F 91486 analogues 141–145. Reagents and conditions: (a) **5** (1 equiv), **28** or **138** (1 equiv), DCM, overnight, 0 °C → rt; (b) K₂CO₃ (2.1 equiv), MeOH/H₂O (7/3, v/v), 3–5 h, rt; (c) 20% TFA, DCM, overnight, reflux; (d) i) 66% HI, EtOH, rt; ii) CH₃I (1.1 equiv), MeOH 1 h, reflux; (e) NaOH (1 M solution), 1 h, reflux.

literature. In this study we resynthesized these structures for further pharmacological investigations.

Pharmacology

The ligands **115**–**136** and **141**–**145** were pharmacologically characterized using radioligand binding assays (*h*H_{1,2,3,4}R), the guinea pig ileum assay (*gp*H₁R) as well as the guinea pig right atrium assay (*gp*H₂R). The most interesting compounds were further investigated in the [³⁵S]GTPγS binding assay (*h*H_{2,3,4}R). The radioassays were performed using membranes of Sf9 cells expressing the respective histamine receptor described in Table 1 and 2.

Introduction of a third basic moiety was the main focus by developing new ligands as shown in Scheme 2. Therefore, we created terminal amines **115**–**122**, guanidines **123**–**131** and

ureas **132**–**136** with different spacer lengths. Furthermore, heterocyclic exchange of imidazole by amino(methyl)thiazole should give more insight in the selectivity profile of the ligands. The compounds depicted in Scheme 3 (**141**–**145**) were mainly altered by heteroatomic exchange at the guanidine group of **2**. The following influence on basicity should give important information about the variability of this partial structure, with respect to histamine receptor affinity and potency.

Radioligand Binding Data

A correlation was found between binding affinities of the amines **115**–**122** at the *h*H₁R and the respective lipophilicity (Table 1). From C₃- (**115**) to C₁₂-spacer (**120**–**122**) there is an upward shift of approximately 3 log units. The tendency at the *h*H₂R is the same, but to a lesser extent. The highest affinity

Table 1. Binding data (pK_i values) of compounds DPH, 1–4, 115–136 and 141–145 determined at human H_xRs ($x=1-4$).^[a]

compound	$hH_1R^{[b]}$ pK_i	N	$hH_2R^{[c]}$ pK_i	N	$hH_3R^{[d]}$ pK_i	N	$hH_4R^{[e]}$ pK_i	N
DPH	7.62 ± 0.01	4	n.d.	–	n.d.	–	n.d.	–
1	5.62 ± 0.03	3	6.58 ± 0.04	48	7.59 ± 0.01	42	7.60 ± 0.01	45
2	< 4	3	5.39 ± 0.04 ^[f]	3	7.42 ± 0.04	3	8.13 ± 0.08	3
3	< 5.5	2	7.33 ± 0.05	3	5.25 ± 0.05	3	5.00 ± 0.05	3
4	< 4.5	2	5.52 ± 0.05	3	7.21 ± 0.02	3	8.04 ± 0.05	3
115	< 4	2	6.63 ± 0.06	3	5.59 ± 0.03	3	7.03 ± 0.07	3
116	< 5	2	6.07 ± 0.04	3	5.82 ± 0.03	3	6.47 ± 0.02	3
117	< 5	2	6.12 ± 0.04	3	6.19 ± 0.01	3	6.36 ± 0.03	3
118	5.91 ± 0.03	2	6.44 ± 0.02	3	6.65 ± 0.04	3	6.33 ± 0.03	3
119	6.06 ± 0.03	2	6.80 ± 0.02	3	7.14 ± 0.01	3	6.78 ± 0.01	3
120	6.71 ± 0.02	2	7.28 ± 0.04	3	7.45 ± 0.02	3	7.16 ± 0.04	3
121	6.30 ± 0.01	2	6.50 ± 0.09	3	5.38 ± 0.01	3	5.33 ± 0.03	3
122	6.52 ± 0.01	2	6.73 ± 0.05	3	5.29 ± 0.06	3	4.65 ± 0.06	3
123	< 4.5	2	6.15 ± 0.05	3	6.41 ± 0.01	3	7.51 ± 0.04	3
124	< 5	2	6.24 ± 0.02	3	6.97 ± 0.03	3	6.62 ± 0.02	3
125	< 5.5	2	6.80 ± 0.10	3	7.20 ± 0.03	3	6.84 ± 0.02	3
126	6.09 ± 0.01	2	6.85 ± 0.06	3	7.43 ± 0.02	3	7.50 ± 0.02	3
127	6.59 ± 0.01	2	7.06 ± 0.04	3	7.48 ± 0.05	3	7.55 ± 0.02	3
128	5.75 ± 0.01	2	6.67 ± 0.01	3	6.53 ± 0.03	3	6.40 ± 0.01	3
129	6.58 ± 0.01	2	7.03 ± 0.09	3	6.25 ± 0.04	3	5.62 ± 0.05	3
130	6.25 ± 0.01	2	6.93 ± 0.02	3	7.07 ± 0.01	3	6.23 ± 0.09	3
131	6.28 ± 0.01	2	6.84 ± 0.05	3	6.43 ± 0.17	3	6.47 ± 0.07	3
132	< 4.5	2	5.75 ± 0.10	3	6.80 ± 0.01	3	6.84 ± 0.01	3
133	< 4.5	2	6.57 ± 0.03	3	6.27 ± 0.05	3	6.59 ± 0.02	3
134	< 5	2	6.55 ± 0.07	3	6.69 ± 0.02	3	6.18 ± 0.03	3
135	< 5.5	2	6.58 ± 0.11	3	6.84 ± 0.02	3	6.56 ± 0.01	3
136	< 5.5	2	6.95 ± 0.02	3	7.00 ± 0.01	3	6.70 ± 0.01	3
141	< 4	2	4.26 ± 0.09	3	6.78 ± 0.05	3	6.82 ± 0.04	3
142	< 4	2	< 4	3	6.07 ± 0.03	3	5.77 ± 0.02	3
143	< 4	2	4.98 ± 0.09	3	6.58 ± 0.08	3	8.14 ± 0.01	3
144	< 4	2	< 4	3	6.09 ± 0.01	3	5.28 ± 0.06	3
145	< 5	2	6.17 ± 0.08	3	6.91 ± 0.03	3	6.83 ± 0.02	3

^[a]Data represent mean values ± SEM from at least two independent experiments (N), each performed in triplicate. Radioligand competition binding experiments performed with ^[b][³H]mepyramine (hH_1R , K_d 4.5 nM, $c=5$ nM), ^[c][³H]tiotidine (hH_2R , K_d 19.7 nM, $c=10$ nM), ^[d][³H]N^α-methylhistamine (hH_3R , K_d 8.6 nM, $c=3$ nM) or ^[e][³H]histamine (hH_4R , K_d 16.0 nM, $c=15$ nM) at membranes of Sf9 cells expressing ^[b]the hH_1R plus RGS4, ^[c]the hH_2R plus $G_s\alpha_s$, ^[d]the hH_3R plus $G\alpha_{i2}$ plus $G\beta_1\gamma_2$, ^[e]the hH_4R plus $G\alpha_{i2}$ plus $G\beta_1\gamma_2$. ^[f]Displacement of [³H]UR-DE257 (hH_2R , K_d 31.3 nM, $c=20$ nM) instead of [³H]tiotidine; n.d. = not determined.

Table 2. Agonistic (pEC_{50}) and antagonistic (pK_B) activities of 1–3, 120, 121, 127, 130 and 136 at the $hH_{2,3,4}R$ determined in the [³⁵S]GTP γ S binding assay.^[a]

Compound	$hH_2R^{[b]}$ $pEC_{50}^{[e]}$	$E_{max}^{[f]}$	N	$hH_3R^{[c]}$ $pEC_{50}^{[e]}$ (pK_B) ^[g]	$E_{max}^{[f]}$	N	$hH_4R^{[d]}$ $pEC_{50}^{[e]}$ (pK_B) ^[g]	$E_{max}^{[f]}$	N
1	6.01 ± 0.07	1.00	7	8.52 ± 0.10	1.00	6	8.20 ± 0.08	1.00	3
2	5.59 ± 0.01 ^{[h],[46]}	0.66 ± 0.02 ^{[h],[46]}	3	8.12 ± 0.10 ^{[h],[46]}	0.69 ± 0.04 ^{[h],[46]}	3	8.09 ± 0.04 ^{[h],[46]}	0.83 ± 0.01 ^{[h],[46]}	3
3	6.61 ± 0.03	0.33 ± 0.03	5	(4.53 ± 0.05)	0	3	(3.83 ± 0.03)	0	3
120	6.95 ± 0.04	0.66 ± 0.01	3	(6.72 ± 0.03)	0	3	(3.43 ± 0.01)	0	3
121	7.11 ± 0.10	0.22 ± 0.01	3	5.88 ± 0.03	−0.69 ± 0.03	3	(3.75 ± 0.01)	0	3
127	6.86 ± 0.03	0.45 ± 0.03	3	(7.18 ± 0.04)	0	3	(3.38 ± 0.01)	0	3
130	7.28 ± 0.10	0.22 ± 0.01	3	4.46 ± 0.02	−1.21 ± 0.10	3	4.52 ± 0.02	−0.98 ± 0.01	3
136	6.72 ± 0.06	0.45 ± 0.03	3	4.57 ± 0.03	−1.20 ± 0.15	3	4.44 ± 0.01	−0.96 ± 0.02	3

^[a]Data represent mean values ± SEM from at least three independent experiments (N), each performed in triplicate. Data were analyzed by nonlinear regression and were best fitted to sigmoidal concentration-response curves (CRCs). [³⁵S]GTP γ S binding assay at membranes of Sf9 cells expressing ^[b]the hH_2R plus $G_s\alpha_s$, ^[c]the hH_3R plus $G\alpha_{i2}$ plus $G\beta_1\gamma_2$, ^[d]the hH_4R plus $G\alpha_{i2}$ plus $G\beta_1\gamma_2$; ^[e] pEC_{50} ; ^[f] E_{max} : maximal response relative to histamine ($E_{max}=1.00$); ^[g]For determination of antagonism, reaction mixtures contained histamine (1) (100 nM) and ligands were at concentrations from 10 nM and 1 mM; $pK_B = -\log K_B$. ^[h]Determined in a steady-state [³²P]GTPase assay on Sf9 cells expressing the related receptors.

value was measured for **120** ($pK_i=7.28$, Table 1). In comparison with compounds bearing small alkylic side chains like UR–Po194 (**4**), showing high affinity at the hH_4R ,^[40] introduction of a terminal amine with similar spacer length (**115**, **116**) led to a remarkable loss in affinity of at least 1 log unit (Table 1). Heterocyclic replacement by amino(methyl)thiazole resulted in the already known affinity decrease at the $hH_{3,4}Rs$. Related to

the hH_2R **121** and **122** reveal moderate selectivity towards the $hH_{3,4}Rs$, but not towards the hH_1R (Table 1).

Data for the guanidines **123–131** at the hH_1R and the hH_2R were similar to those of the amines **115–122**. Increasing spacer length led to higher affinity values culminating in **127** (pK_i (hH_1R) = 6.59; pK_i (hH_2R) = 7.06; cf. Table 1). Affinity values at the $hH_{3,4}Rs$ were all in a submicromolar range and this time a switch

from imidazole to amino(methyl)thiazole resulted in a moderate affinity loss from maximally 1 log unit, which is noticeably low. A slight selectivity vis-à-vis hH_2R and $hH_{1,3,4}Rs$ is just seen for **129** (Table 1). All further compounds revealed similar but partially high affinities, especially for the $hH_{2,3,4}Rs$.

Introducing a terminal urea in the side chain (**132**–**136**) comes along with a massive decrease in basicity, but not with a massive loss in affinity. Overall they were in a range with the terminal amines (**115**–**122**) and guanidines (**123**–**131**), which means slight or no affinity at the hH_1R and submicromolar affinities at the $hH_{2,3,4}Rs$ (Table 1). This functionality has no remarkable impact or change with respect to selectivity or affinity at the histamine receptors.

Compounds **141**–**145** with its nonlipophilic structures presented – as expected – no affinity for the hH_1R (Table 1). Values at the hH_2R were similar, instead of **145**, where the urea analogue of **2** surprisingly demonstrated higher affinity (pK_i (**145**) = 6.17; pK_i (**2**) = 5.39; cf. Table 1). Scoping at the $hH_{3,4}Rs$ the benzoyl derivatives **141** and **144** illustrated moderate binding values. Even if the affinities of **141** at the $hH_{3,4}Rs$ were higher, **144** tends to be selective towards the hH_3R (Table 1). Compound **143** gives an even more pronounced selectivity towards the hH_4R (Figure 3). Besides the weak binding data at the $hH_{1,2}Rs$ and a moderate result at the hH_3R (pK_i (hH_3R) = 6.58), a pK_i of 8.14 showed up a remarkably high tendency for the hH_4R (Table 1). In comparison with the binding data of **2**, the selectivity profile of the *S*-methylated analogue **143** has improved.

$[^{35}S]GTP\gamma S$ Binding Data

The functional data of the $[^{35}S]GTP\gamma S$ assay characterize **120** as a partial agonist at the hH_2R (pEC_{50} = 6.95) and an intrinsic activity of 66%, relative to histamine (Table 2). At the hH_3R an antagonistic activity (pK_B = 6.72) of **120** could be measured, as well as a negligible weak antagonistic effect at the hH_4R (Table 2). The values for **121** were quite similar. The partial

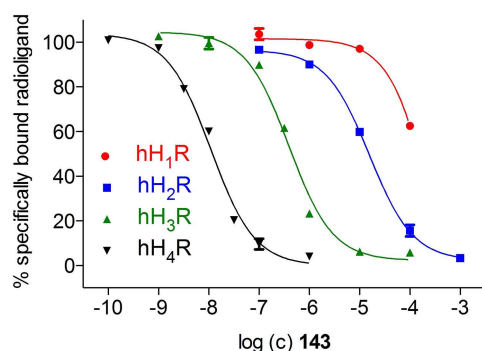


Figure 3. Selectivity profile of **143** with radioligand displacement curves from radioligand binding assays. Experiments were performed with compound **143** and $[^3H]$ mepyramine (hH_1R , K_d 4.5 nM, c = 5 nM), $[^3H]$ tiotidine (hH_2R , K_d 19.7 nM, c = 10 nM), $[^3H]N^m$ -methylhistamine (hH_3R , K_d 8.6 nM, c = 3 nM) or $[^3H]$ histamine (hH_4R , K_d 16.0 nM, c = 15 nM) at membranes of Sf9 cells expressing the respective hHR . Data represent mean values \pm SEM from at least two independent experiments, each performed in triplicate.

agonism at the hH_2R is equipotent, but less effective (E_{max} = 0.22) and functionality at the hH_3R turns into a partial inverse agonism at one digit micromolar range (Table 2). **120** and **121** are just different in its heterocyclic group (imidazole vs. aminomethylthiazole).

The same structural decision was made for further characterization of terminal guanidines. **127** and **130** both bear a C_{12} -chain with different heterocyclic cycles. Compared to the amines, functional data were similar and in accordance with binding data (Table 2). **130** is a partial agonist at the hH_2R (pEC_{50} = 7.28, E_{max} = 0.22) and a weak but full inverse agonist at the $hH_{3,4}Rs$, while **127** acts as a silent antagonist at these receptors (Table 2). The switch from antagonism to inverse agonism at the $hH_{3,4}Rs$ could be assigned to the aminomethylthiazole structure.

The functional experiments of the urea analogue **136** were in line with these data. Partial agonism (pEC_{50} = 6.72, E_{max} = 0.45) at the hH_2R , as well as a (partial) inverse agonism at the $hH_{3,4}Rs$ could be measured (Table 2). **136** was the only imidazole-containing compound, that shows up an (partial) inverse agonism at these receptors.

Organ Pharmacological Data

Data from organ bath studies at the guinea pig ileum (gpH_1R) and right atrium (gpH_2R) provided functional values under physiological conditions. The class of terminal amines (**115**–**122**) showed a steady increase in their antagonistic activity at the gpH_1R by elongation of the alkyl side chain (pA_2 (**115**–**120**) = 4.78–6.95; cf. Table 3). A further significant increase could be observed by exchange of the heterocycle by aminothiazole (pA_2 (**122**) = 8.03; cf. Table 3). Agonistic data at the gpH_2R gave potencies in a submicromolar range with high intrinsic activities culminated in **120** as a full agonist (pEC_{50} = 6.86, E_{max} = 1.00; cf. Table 3). Heterocyclic exchange with amino(methyl)thiazoles led to a slight decrease in potency and efficacy.

The raise of basicity, with respect to the terminal guanidines (**123**–**131**), resulted in slightly higher antagonistic values at the gpH_1R compared to the respective amines (e.g. pA_2 (**127**) = 7.22; cf. Table 3). In analogy to **122**, substitution of imidazole by aminothiazole led to a highly active antagonist at the gpH_1R (pA_2 (**131**) = 8.06; cf. Table 3). Terminal guanidines (**123**–**131**) were developed to more potent and highly efficient agonists at the gpH_2R , in comparison to their amine and alkyl analogues (the latter were published by Pockes et al.^[40]). However, it is striking that the alkylic spacer length seems to have no significant influence on the agonistic potency (Table 3). The most potent guanidine **125** (pEC_{50} = 7.69, E_{max} = 0.83) and the most efficient guanidine **123** (pEC_{50} = 7.30, E_{max} = 1.03) bear a C_8 - and a C_4 -spacer, respectively (Table 3).

Organ pharmacological data for the ureas **132**–**136** were in comparison with the respective amines **115**–**122** (Table 3). Therefore, **135** and **136** with its lipophilic C_8 - and C_{10} -spacer, respectively, pointed up highest antagonistic activity at the gpH_1R (pA_2 (**135**) = 5.85; pA_2 (**136**) = 6.00; cf. Table 3). All compounds, instead of **132**, exhibited values in a submicromo-

Table 3. Agonistic (pEC_{50}) and antagonistic (pA_2) activities of 1–4, 115–136 and 141–145 determined by organ bath studies at the gpH_1R (ileum) and the gpH_2R (atrium).^[a]

Compound	gpH_1R pA_2 ^[b] (pEC_{50})	<i>N</i>	gpH_2R pEC_{50} ^{[c],[d]}	E_{max} ^[e]	<i>N</i>
1	(6.68 ± 0.03)	255	6.16 ± 0.01	1.00	225
2	n.a. ^f	24	5.16 ± 0.04	0.75 ± 0.03	5
3	5.88 ± 0.03	9	8.38 ± 0.05	0.78 ± 0.01	3
4	4.83 ± 0.05	8	5.40 ± 0.11	0.83 ± 0.03	3
115	4.78 ± 0.02	8	5.33 ± 0.11	0.88 ± 0.05	3
116	5.42 ± 0.05	9	5.13 ± 0.05	0.68 ± 0.02	3
117	5.20 ± 0.07	9	6.42 ± 0.08	0.79 ± 0.01	3
118	5.89 ± 0.05	9	6.51 ± 0.05	0.75 ± 0.10	3
119	6.17 ± 0.04	9	6.41 ± 0.05	0.78 ± 0.01	3
120	6.95 ± 0.06	9	6.86 ± 0.06	1.00 ± 0.06	3
121	7.15 ± 0.06	8	6.49 ± 0.09	0.71 ± 0.03	3
122	8.03 ± 0.03	15	6.63 ± 0.07	0.90 ± 0.05	3
123	5.58 ± 0.02	6	7.30 ± 0.05	1.03 ± 0.03	3
124	6.03 ± 0.04	6	7.67 ± 0.03	0.94 ± 0.02	3
125	5.79 ± 0.03	6	7.69 ± 0.02	0.83 ± 0.07	3
126	6.60 ± 0.04	6	7.56 ± 0.04	0.80 ± 0.02	3
127	7.22 ± 0.05	6	7.25 ± 0.11	0.77 ± 0.07	3
128	6.67 ± 0.04	6	6.87 ± 0.04	0.72 ± 0.02	3
129	7.30 ± 0.05	6	7.41 ± 0.09	1.00 ± 0.01	3
130	6.76 ± 0.05	6	7.02 ± 0.07	0.90 ± 0.04	3
131	8.06 ± 0.05	14	6.93 ± 0.09	0.85 ± 0.05	3
132	5.04 ± 0.04	6	5.61 ± 0.08	0.89 ± 0.03	3
133	5.22 ± 0.08	6	6.54 ± 0.08	1.03 ± 0.03	3
134	5.13 ± 0.04	4	6.17 ± 0.09	0.96 ± 0.03	3
135	5.85 ± 0.04	6	6.74 ± 0.09	0.94 ± 0.05	3
136	6.00 ± 0.03	6	6.53 ± 0.01	0.96 ± 0.01	3
141	n.a. ^f	12	4.73 ± 0.05	0.43 ± 0.01	3
142	n.a. ^f	9	4.96 ± 0.08	0.27 ± 0.02	3
143	5.41 ± 0.06	6	5.13 ± 0.03	0.45 ± 0.05	3
144	5.02 ± 0.06	6	4.62 ± 0.05	0.15 ± 0.03	3
145	< 4.5	6	3.57 ± 0.02	0.58 ± 0.02	3

^[a]Data represent mean values ± SEM from at least three independent experiments (*N*). Data were analyzed by nonlinear regression and were best fitted to sigmoidal concentration-response curves. ^[b] pA_2 : $-\log c(\text{Ant}) + \log(r-1)$; $r = 10^{\Delta pEC_{50}}$; ΔpEC_{50} was calculated from pEC_{50} of histamine and pEC_{50} of histamine in presence of the respective antagonist; ^[c] pEC_{50} : $-\log EC_{50}$; ^[d] pEC_{50} was calculated from the mean corrected shift ΔpEC_{50} of the agonist curve relative to the histamine reference curve by equation $pEC_{50} = 6.16 + \Delta pEC_{50}$; ^[e] E_{max} : maximal response relative to the maximal increase in heart rate induced by histamine ($E_{max} = 1.00$). ^[f]n.d. = not determined.

lar range at the gpH_2R with remarkable high agonistic efficacy ($E_{max} = 0.89$ – 1.03 ; cf. Table 3).

Compounds 141–145 boasted only slight or no antagonistic activity at the gpH_1R (Table 3). Compared to 2, which reveals a guanidine structure, the less basic thiourea (141, 142) and urea derivatives (144, 145) presented weak partial agonism at the guinea pig right atrium (gpH_2R). Isothiourea 143 is equipotent ($pEC_{50} = 5.13$) but less effective ($E_{max} = 0.45$) referred to SK&F 91486 (2). According to the literature 143 demonstrated a potency comparable to histamine (rel. potency = 0.1) at the guinea-pig right atrium, while the maximum response was higher (0.45 vs. 0.23).^[35]

The maximum responses of the tested compounds (115–136 and 141–145) at the right atrium were completely antagonized after addition of the H_2R antagonist cimetidine ($pA_2 = 6.10$ ^[58,59]) (30 μM). For compounds 120, 125 (Figure S35, Supporting Information (SI)) and 135 full concentration-response curves (CRCs) in the presence of cimetidine (30 μM , 30 min preincubation) were determined. The presence of an antagonist resulted in rightward shifted curves. The calculated values via Schild equation (Table S2, SI) were in accordance with the experimental data. This outcome confirms that the incre-

ment of the heart frequency in the guinea-pig right atrium assay was conveyed via the H_2R . The most interesting results at the gpH_2R were displayed in Figure 4, where CRCs of selected

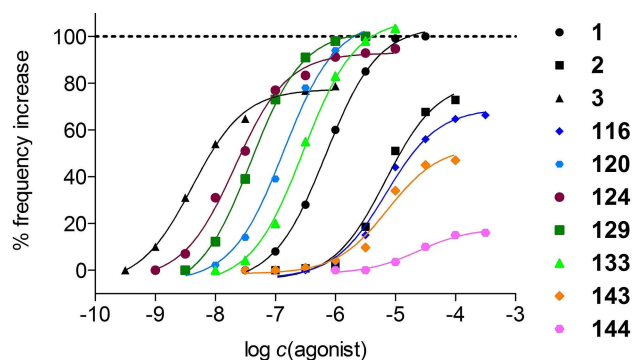


Figure 4. Concentration-response curves of 1, 2 and 3 (black), as well as 116, 120, 124, 129, 133, 143 and 144 (colored) at the gpH_2R (atrium). Histamine (1) was used as a reference ($pEC_{50} = 6.16$, $E_{max} = 1.00$). Displayed curves are calculated by endpoint determination ($N = 1$).

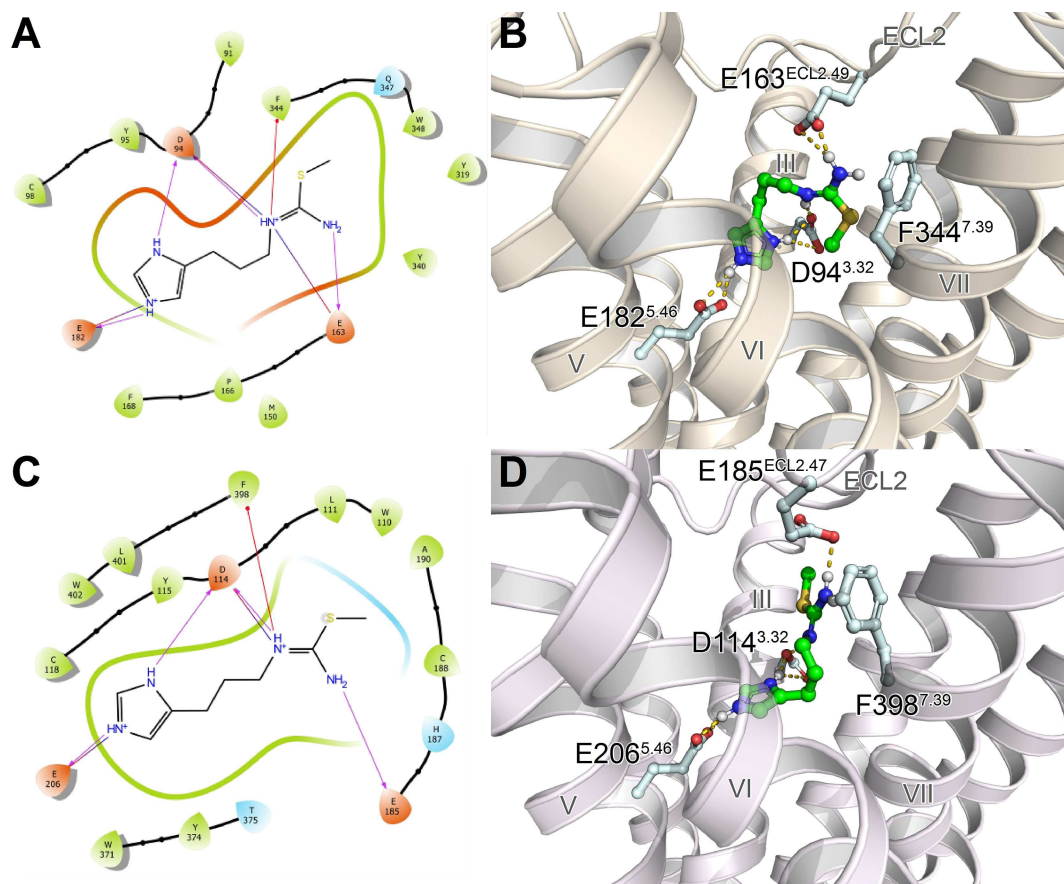


Figure 5. Lowest free energy (MM-GBSA) docking poses of **143** at both the hH_4R (A, B) and hH_3R (C, D) showing key ligand-receptor interactions in the form of ligand interaction diagrams (A, C) or three-dimensional illustrations (B, D). Hydrogen bonds and salt bridges are colored in magenta (A, C) or yellow (B, D), and cation- π interactions in red (A, C).

compounds of each group (colored) were depicted together with references (black).

Computational Studies

143 was “flexibly” docked into the orthosteric binding pocket of both the hH_4R and hH_3R (cf. Figure 5), two closely related histamine receptor subtypes sharing a high sequence identity.^[15,60] Of the investigated protonation and/or tautomerization states of the imidazole ring (τ -H and π -H, τ -H, π -H), docking of **143** resulted in the most reasonable binding poses and in the lowest MM-GBSA values in case of the protonated (τ -H and π -H) form of the imidazole ring. At first, ligand-receptor interactions of these lowest free energy (MM-GBSA) binding poses seemed to be highly comparable between both histamine receptor subtypes (cf. Figure 5): The isothiourea moiety and the protonated imidazole ring of **143** formed salt bridges with D94^{3.32}, E163^{ECL2.49} and E182^{5.46} (hH_4R) or D114^{3.32}, E185^{ECL2.47} and E206^{5.46} (hH_3R). In addition, cation- π -interactions were detected between the isothiourea moiety of **143** and F344^{7.39} (hH_4R) or F398^{7.39} (hH_3R). However, by taking a closer look at the differences between binding of **143** to either hH_4R or hH_3R , it becomes obvious that the location of a certain GLU

in the extracellular loop 2 (hH_4R : E163^{ECL2.49}, hH_3R : E185^{ECL2.47}) is shifted by two amino acids. Therefore, the orientation of this GLU residue seems to slightly differ between both receptor subtypes: Whereas it seems to be still capable of properly forming a salt bridge with the isothiourea moiety of **143** in case of the hH_4R , the interactions may be weakened in the case of hH_3R . Furthermore, this salt bridge appeared in four of five docking poses in case of the hH_4R compared to only one of five in case of the hH_3R . Consequently, these molecular differences may, at least in parts, reflect the discrepancies in pK_i values of more than one order of magnitude between hH_4R and hH_3R (hH_4R : $pK_i = 8.14$, hH_3R : $pK_i = 6.58$, cf. Table 1) and thus provide a possible molecular explanation.

Conclusions

Novel series of alkylated hetarylpropylguanidines with functionalized side chains or new functionality at the guanidine structure were investigated in this project. By introduction of three different functional groups (amine, guanidine, urea) in a terminal position of an alkylic side chain various shades of basicity could be displayed. The respective ligands **115**–**136** were obtained in a six- to nine-step synthesis in excellent yield,

just as for compounds **141–145** (two to three steps). Elongation of the spacer length and, associated therewith, the increase of lipophilicity led to higher affinities and potencies at all four histamine receptors. The most affine and potent derivatives (two digit nanomolar range) could be assigned to guanidines in the terminal position (**123–131**), in comparison with the appropriate amines (**115–122**) and ureas (**132–136**). None of these classes pointed up a distinct selectivity towards any of the four histamine receptors. Although bioisosteric replacement of imidazole by amino(methyl)thiazole led to selectivity towards the H_2R , improvement of the selectivity profile could not be determined, in comparison with already described H_2 -selective compounds. Heteroatomic exchange at the guanidine group of SK&F 91486 (**2**) led to benzoylurea derivative **144**, with a preference towards the hH_3R , and isothioureas **143**, with considerable improvement of the selectivity profile towards the hH_4R . Thereby, computational studies provided molecular insights into the binding modes of **143** at both hH_4R and hH_3R and supported the proposal of a possible mechanism of the enhanced selectivity profile. Furthermore, both structures, **143** and **144**, could be an interesting starting point for future projects facing H_3 and H_4 receptor selectivity. This is of special interest as to date there are still no drugs available for both receptors (apart from Pitolisant^[61]), although a wide field of applications are reported for the H_3R (e.g. several neurodegenerative diseases)^[21–25] and the H_4R (e.g. inflammation, allergic diseases).^[26–30]

Experimental Section

General Conditions

Commercially chemicals (**8**, **11–16**, **28** and **138**), reagents and solvents were purchased from Acros Organics (Geel, Belgium), Alfa Aesar GmbH & Co. KG (Karlsruhe, Germany), Iris Biotech GmbH (Marktredwitz, Germany), Merck KGaA (Darmstadt, Germany), Sigma-Aldrich Chemie GmbH (München, Germany) or TCI Europe (Zwijndrecht, Belgium) and were used as received. Deuterated solvents for nuclear magnetic resonance (1H NMR and ^{13}C NMR) spectra were purchased from Deutero GmbH (Kastellaun, Germany). All reactions including dry solvents were carried out in dry flasks under nitrogen or argon atmosphere. For the preparation of buffers, HPLC eluents and stock solutions millipore water was used. Column chromatography was accomplished using Merck silica gel Geduran 60 (0.063–0.200 mm) or Merck silica gel 60 (0.040–0.063 mm) (flash column chromatography). Reactions were monitored by TLC on aluminium sheets with silica gel 60 F_{254} from Merck. Spots were detected under UV light at 254 nm, by iodine vapor, ninhydrin or fast blue B staining. Nuclear magnetic resonance (1H NMR and ^{13}C NMR) spectra were measured on a Bruker (Karlsruhe, Germany) Avance 300 (1H : 300 MHz, ^{13}C : 75 MHz) or Avance 400 (1H : 400 MHz, ^{13}C : 101 MHz) spectrometer using perdeuterated solvents. Chemical shifts (δ) are given in parts per million (ppm). Multiplicities were stated using the following abbreviations: s (singlet), d (doublet), t (triplet), q (quartet), p (pentet), m (multiplet) and bs (broad signal) and combinations thereof. ^{13}C NMR-Peaks were measured by DEPT 135 and DEPT 90 (distortionless enhancement by polarization transfer): “+” primary and tertiary carbon atom (positive DEPT 135 signal), “-” secondary carbon atom (negative DEPT 135 signal), “quat” quaternary carbon

atom. NMR spectra were processed with MestReNova 11.0 (Mestrelab Research, Compostela, Spain). High resolution mass spectrometry (HRMS) was performed on an Agilent 6540 UHD Accurate-Mass Q-TOF LC/MS system (Agilent Technologies, Santa Clara, CA) using an ESI source. Elemental analyses (EA) were executed on a Heraeus Elementar Vario EL III and are within $\pm 0.4\%$ unless otherwise noted. Melting points (mp) were detected on a Büchi (Essen, Germany) B-545 apparatus using an open capillary and are uncorrected. Preparative HPLC was handled with a system from Knauer (Berlin, Germany) consisting of two K-1800 pumps and a K-2001 detector. A Eurospher-100 C18 (250 \times 32 mm, 5 μ m) (Knauer, Berlin, Germany) or a Kinetex XB-C18 (250 \times 21.2 mm, 5 μ m) (Phenomenex, Aschaffenburg, Germany) served as stationary phase. As mobile phase, 0.1% TFA in millipore water and acetonitrile (MeCN) were used. The temperature was 25 °C, the flow rate 15 mL/min and UV detection was performed at 220 nm. Analytical HPLC was implemented on an Agilent 1100 HPLC system (Agilent Technologies, Santa Clara, CA) using a binary pump, autosampler, and DAD detector. Stationary phase was a Kinetex XB-C18 (250 \times 4.6 mm, 5 μ m) (Phenomenex, Aschaffenburg, Germany). As mobile phase, mixtures of MeCN and aqueous TFA were used (linear gradient: MeCN/TFA (0.1%) (v/v) 0 min: 5:95, 25 min: 50:50, 26–35 min: 95:5 (method A); flow rate = 1.0 mL/min, t_0 = 2.57 min). Capacity factors were calculated pursuant to $k = (t_R - t_0)/t_0$. Detection was measured at 220 nm. All compounds were examined using method A. Filtration of the stock solutions with PTFE filters (25 mm, 0.2 μ m, Phenomenex Ltd., Aschaffenburg, Germany) was carried out before testing. Compound purities determined by HPLC were calculated as the peak area of the analyzed compound in % relative to the total peak area (UV detection at 220 nm). The HPLC purities (see analytical data and Supporting Information) of the final compounds were $\geq 95\%$. For all purity runs (see SI) the blank run was subtracted to avoid TFA-dependent baseline drift. All the tested compounds were screened for PAINS and aggregation by publicly available filters (<http://zinc15.docking.org/patterns/home>, <http://advisor.docking.org>).^[62,63] None of the screened molecules have been previously reported as PAINS or an aggregator. Since Devine et al. described 2-aminothiazoles as a promiscuous frequent hitting scaffold at different enzymes,^[64] full dose response curves for all experiments and compounds – not only for the 2-aminothiazoles – were performed. None of the curves displayed abnormalities, e.g. high Hill slopes, what could be an indication for PAINS.^[63]

Chemical Synthesis and Analytical Data

General Procedure for the Preparation of the Mono-Boc-Protected Diamines 17–22

A 0.5 M solution of Boc_2O (1 equiv) in DCM was added dropwise over a 2 h period to a 0.25 M solution of diamine **11–16** (5 equiv) in DCM cooled with an ice-bath. The reaction mixture was stirred overnight at room temperature (rt) and filtered. The filtrate was concentrated under vacuum and the resulting oil dissolved in EtOAc was washed with half-saturated brine (3 \times 150 mL), dried (Na_2SO_4) and concentrated under vacuum. The crude product was purified by column chromatography (DCM/MeOH/7 M NH_3 in MeOH 80/18/2 – 50/48/2 v/v/v).

N-(*tert*-Butoxycarbonyl)-1,3-propanediamine (**17**)^[49]

The reaction was carried out with propane-1,3-diamine (**11**, 3.83 mL, 45.87 mmol), Boc_2O (2.0 g, 9.16 mmol) and DCM. The product was obtained as a colorless oil (1.55 g, 97%); R_f = 0.40 (DCM/MeOH/ NH_3 80:20:0.1); 1H NMR (300 MHz, $CDCl_3$) δ 5.06 (t, J =

5.3 Hz), 3.20 (q, $J=6.2$ Hz, 2H), 2.86 (bs, 2H), 2.79 (t, $J=6.6$ Hz, 2H), 1.65 (p, $J=6.6$ Hz, 2H), 1.43 (s, 9H). ^{13}C NMR (75 MHz, CDCl_3) δ 156.23, 79.15, 39.17, 38.19, 32.55, 28.42. HRMS (ESI-MS): m/z [$\text{M} + \text{H}^+$] calculated for $\text{C}_8\text{H}_{19}\text{N}_2\text{O}_2^+$: 175.1441, found 175.1445; $\text{C}_8\text{H}_{18}\text{N}_2\text{O}_2$ (174.24).

General Procedure for the Preparation of the *N*-Aminoalkyl-*N,N'*-di-Boc-Protected Guanidines 23–27

A solution of **10** (1 equiv) in DCM (50 mL) was added dropwise to a solution of the respective diamine (**12–16**, 3 equiv) in DCM (50 mL) at rt. The resulting mixture was stirred over night and washed with H_2O (3x25 mL) and brine (30 mL). The organic solvent was dried over Na_2SO_4 and the crude product was purified with column chromatography (DCM/MeOH/7 M NH_3 in MeOH 95/3/2 – 90/8/2 v/v).

1-(4-Aminobutyl)-2,3-(di-*tert*-butoxycarbonyl)guanidine (**23**)^[50]

The synthesis was accomplished with **12** (1.37 g, 15.51 mmol) and **10** (1.50 g, 5.17 mmol) according to the general procedure. Column chromatography gave **23** as a yellow oil (1.18 g, 69%): $R_f=0.18$ (DCM/MeOH/ NH_3 95:5:0.1); ^1H NMR (300 MHz, CDCl_3) δ 11.47 (bs, 1H), 8.33 (bs, 1H), 3.39 (q, $J=7.3$ Hz, 2H), 2.71 (t, $J=6.8$ Hz, 2H), 1.86 (bs, 2H), 1.66 – 1.50 (m, 4H), 1.48 (s, 9H), 1.47 (s, 9H). ^{13}C NMR (75 MHz, CDCl_3) δ 163.55, 156.16, 153.30, 83.13, 79.32, 41.60, 40.63, 30.56, 28.29, 28.07, 26.36. HRMS (ESI-MS): m/z [$\text{M} + \text{H}^+$] calculated for $\text{C}_{15}\text{H}_{31}\text{N}_4\text{O}_4^+$: 331.2340, found 331.2346; $\text{C}_{15}\text{H}_{30}\text{N}_4\text{O}_4$ (330.43).

General Procedure for the Preparation of the Benzoylthioureas 29–39

To an ice-cold solution of the pertinent amine (**11–27**, 1 equiv) in DCM, benzoyl isothiocyanate (**28**, 1 equiv) was added dropwise. The reaction was allowed to stir at room temperature (rt) for 2 h. The reaction mixture was washed three times with H_2O and saturated solution of NaCl (each 30 mL). The organic layer was dried over Na_2SO_4 and the crude product was purified with column chromatography (DCM/MeOH 100/0 – 98/2 v/v).

tert-Butyl [3-(3-benzoylthioureido)propyl]carbamate (**29**)^[55]

The product was developed using **17** (1.55 g, 8.90 mmol) and **28** (1.20 mL, 8.90 mmol) in DCM (30 mL) and the desired compound was isolated as a yellow oil (2.91 g, 97%): $R_f=0.15$ (DCM); ^1H NMR (300 MHz, CDCl_3) δ 10.83 (bs, 1H), 9.12 (bs, 1H), 7.91–7.74 (m, 2H), 7.56–7.32 (m, 3H), 5.05 (bs, 1H), 3.77 (q, $J=6.5$ Hz, 2H), 3.21 (q, $J=7.4$ Hz, 2H), 1.86 (p, $J=6.6$ Hz, 2H), 1.42 (s, 9H). ^{13}C NMR (75 MHz, CDCl_3) δ 180.25, 166.91, 156.20, 133.56, 131.74, 129.10, 127.51, 79.50, 42.95, 37.06, 30.20, 28.41. HRMS (ESI-MS): m/z [$\text{M} + \text{Na}^+$] calculated for $\text{C}_{16}\text{H}_{23}\text{N}_3\text{NaO}_3\text{S}^+$: 360.1352, found 360.1355; $\text{C}_{16}\text{H}_{23}\text{N}_3\text{O}_3\text{S}$ (337.44).

The synthesis of **40–44** is described in the literature (cf. **17–21**)^[40] and was carried out with the appropriate diamine **11–15** (1 equiv) and **28** (2 equiv).

General Procedure for the Preparation of the Thioureas 45–55

The general procedure for the synthesis of the thioureas is described in the literature (cf. 4.2.9.)^[40]. The NMR peak splitting due to thione-thiol tautomerism – described in the reference – also appears for the compounds **45–55**.

tert-Butyl (3-thioureidopropyl)carbamate (**45**)^[65]

45 was made out of **29** (2.90 g, 8.59 mmol) and K_2CO_3 (2.49 g, 18.04 mmol) in 50 ml MeOH/ H_2O (7/3 v/v) yielding a yellow oil (1.90 g, 95%): $R_f=0.29$ (DCM/MeOH 95:5); ^1H NMR (300 MHz, CDCl_3) δ 7.42 (bs, 1H), 6.39 (bs, 1H), 5.24 (bs, 1H), 3.56 + 3.25 (2 bs, 1.4H + 0.6H (thione-thiol tautomerism)), 3.13 (q, $J=6.4$ Hz, 2H), 1.80 – 1.61 (m, 2H), 1.39 (s, 9H). ^{13}C NMR (75 MHz, CDCl_3) δ 183.31, 156.80, 79.72, 41.87, 37.38, 29.73, 28.43. HRMS (ESI-MS): m/z [$\text{M} + \text{H}^+$] calculated for $\text{C}_9\text{H}_{20}\text{N}_3\text{O}_2\text{S}^+$: 234.1271, found 234.1271; $\text{C}_9\text{H}_{19}\text{N}_3\text{O}_2\text{S}$ (233.33).

The synthesis of **56–60** is described in the literature (cf. **23–27**)^[40] and was carried out with the appropriate dibenzoylthiourea **40–44** (1 equiv) and K_2CO_3 (4.1 equiv).

General Procedure for the Preparation of the *S*-methylisothioureas 61–71

The general procedure for the synthesis of the *S*-methylisothioureas is described in the literature (cf. 4.2.10.)^[40]

tert-Butyl {3-[(imino(methylthio)methyl)amino]propyl} carbamate (**61**)^[66]

Compound **45** (1.80 g, 7.71 mmol) was dissolved in MeCN (30 mL) and treated with methyl iodide (0.53 mL, 8.49 mmol) resulting a yellow oil (**61** x HI, 2.80 g, 97%): $R_f=0.14$ (DCM/MeOH 95:5); ^1H NMR (300 MHz, CDCl_3 , hydrogen iodide) δ 3.76–3.32 (m, 2H), 3.21 (q, $J=6.3$ Hz, 2H), 2.76 (s, 3H), 1.88 (p, $J=6.6$ Hz, 2H), 1.39 (s, 9H). ^{13}C NMR (75 MHz, CDCl_3 , hydrogen iodide) δ 170.17, 154.28, 78.25, 40.17, 35.13, 26.66, 26.37, 13.41. HRMS (ESI-MS): m/z [$\text{M} + \text{H}^+$] calculated for $\text{C}_{10}\text{H}_{22}\text{N}_3\text{O}_2\text{S}^+$: 248.1427, found 248.1429; $\text{C}_{10}\text{H}_{21}\text{N}_3\text{O}_2\text{S}$ x HI (375.27).

The synthesis of **72–76** is described in the literature (cf. **29–33**)^[40] and was carried out with the appropriate bithiourea **56–60** (1 equiv) and methyl iodide (2.1 equiv).

General Procedure for the Preparation of the *N'*-Boc-*S*-methylisothioureas 77–87

The general procedure for the synthesis of the *N'*-Boc-*S*-methylisothioureas is described in the literature (cf. 4.2.11.)^[40]

tert-Butyl {3-[[[(*tert*-butoxycarbonyl)imino](methylthio)methyl]amino]propyl}carbamate (**77**)

The reaction was realized with **61** (2.70 g, 7.19 mmol), NEt_3 (1.00 mL, 7.19 mmol) and Boc_2O (1.57 g, 7.19 mmol). After column chromatography a colorless oil (2.30 g, 92%) was obtained: $R_f=0.41$ (DCM/MeOH 98:2); ^1H NMR (300 MHz, CDCl_3) δ 9.52 (bs, 1H), 4.61 (bs, 1H), 3.31 (t, $J=7.1$ Hz, 2H), 3.12 (q, $J=7.2$ Hz, 2H), 2.39 (s, 3H), 1.73 (p, $J=6.7$ Hz), 1.43 (s, 9H), 1.37 (s, 9H). ^{13}C NMR (75 MHz, CDCl_3) δ 173.55, 162.07, 156.11, 79.34, 79.20, 41.13, 37.75, 29.96, 28.37, 28.21, 13.65. HRMS (ESI-MS): m/z [$\text{M} + \text{H}^+$] calculated for $\text{C}_{15}\text{H}_{30}\text{N}_3\text{O}_4\text{S}^+$: 348.1952, found 348.1952; $\text{C}_{15}\text{H}_{29}\text{N}_3\text{O}_4\text{S}$ (347.47).

The synthesis of **88–92** is described in the literature (cf. **35–39**)^[40] and was carried out with the appropriate isothiourea **72–76** (1 equiv), NEt_3 (2 equiv) and Boc_2O (2 equiv).

General Procedure for the Guanidinylation reaction of 93–109

To a suspension of the pertinent amine **5**, **6**, or **7** (1 equiv), the pertinent *N*'-Boc-*S*-methylisothiurea **77–87** (1 equiv) and HgCl₂ (1 equiv) in DCM, NEt₃ (3 equiv) was added. The mixture was stirred overnight at rt. A possible excess of HgCl₂ was quenched with 7 N NH₃ in MeOH (3–5 mL). The resulting suspension was filtered over Celite and the crude product was purified with column chromatography (DCM/MeOH/7N NH₃ in MeOH 98/1/1 – 95/3/2 v/v/v).

2-*tert*-Butoxycarbonyl-1-(*N*-*tert*-butoxycarbonylamino)propyl-3-[3-(1-trityl-1*H*-imidazol-4-yl)propyl]guanidine (**93**)

Compound **93** was prepared from **5** (500 mg, 1.36 mmol), **77** (473 mg, 1.36 mmol), HgCl₂ (369 mg, 1.36 mmol) and NEt₃ (0.57 mL, 4.08 mmol) in DCM (20 mL) conforming to the general procedure yielding a yellow foaml like solid (420 mg, 46%): *R*_f = 0.30 (DCM/MeOH/NH₃ 98:2:0.1); ¹H NMR (300 MHz, CDCl₃) δ 9.05 (bs, 1H) 7.42–7.27 (m, 10H), 7.15–7.07 (m, 6H), 6.56 (d, *J* = 0.8 Hz, 1H), 5.91 (bs, 1H), 3.55–3.16 (m, 4H), 3.09 (q, *J* = 5.6 Hz, 2H), 2.56 (t, *J* = 6.3 Hz, 2H), 1.87 (p, *J* = 6.7 Hz, 2H), 1.67–1.48 (m, 2H), 1.44 (s, 9H), 1.41 (s, 9H). ¹³C NMR (75 MHz, CDCl₃) δ 164.20, 160.89, 156.55, 142.34, 140.46, 138.02, 129.72, 128.12, 128.10, 118.31, 78.74, 75.26, 75.24, 40.23, 40.20, 36.93, 33.15, 30.58, 29.16, 28.57, 28.51. HRMS (ESI-MS): *m/z* [M + H⁺] calculated for C₃₉H₅₁N₆O₄⁺: 667.3966, found 667.3970; C₃₉H₅₀N₆O₄ (666.87).

General Procedure for the Guanidinylation Reaction of 110–114

To a suspension of the amine **5** (2 equiv), the pertinent *N*'-Boc-*S*-methylisothiurea **88–92** (1 equiv) and HgCl₂ (4 equiv) in DCM, NEt₃ (6 equiv) was added. The mixture was stirred overnight at rt. A possible excess of HgCl₂ was quenched with 7 N NH₃ in MeOH (3–5 mL). The resulting suspension was filtered over Celite and the crude product was purified with column chromatography (DCM/MeOH/7 N NH₃ in MeOH 98/1/1 – 95/3/2 v/v/v).

2-*tert*-Butoxycarbonyl-1-(*N*'-*tert*-butoxycarbonylcarbodiimidopropyl)-3-[3-(1-trityl-1*H*-imidazol-4-yl)propyl]guanidine (**110**)

Compound **110** was prepared from **5** (1.0 g, 2.72 mmol), **88** (572 mg, 1.36 mmol), HgCl₂ (1.48 g, 5.44 mmol) and NEt₃ (1.13 mL, 8.16 mmol) in DCM (20 mL) conforming to the general procedure yielding a yellow oil (430 mg, 46%): *R*_f = 0.44 (DCM/MeOH/NH₃ 98:2:0.1); ¹H NMR (300 MHz, CDCl₃) δ 9.75 (bs, 1H), 7.34–7.21 (m, 10H), 7.14–7.03 (m, 6H), 6.51 (s, 1H), 3.52–3.08 (m, 6H), 2.68–2.46 (m, 2H), 1.99–1.71 (m, 4H), 1.41 (s, 9H), 1.39 (s, 9H). ¹³C NMR (75 MHz, CDCl₃) δ 164.45, 160.71, 158.01, 156.00, 142.52, 140.58, 138.41, 129.73, 128.00, 127.94, 117.91, 85.50, 78.63, 75.02, 53.52, 45.56, 43.58, 28.54, 28.26, 27.93, 25.78, 21.06. MS (LC-MS, ESI): *m/z* 692.39 [M + H⁺]; C₄₀H₄₉N₇O₄ (691.88).

General Procedure for the Preparation of the Title Compounds 115–136

The general procedure for the synthesis of **115–136** is described in the literature (cf. 4.2.7).^[40] All compounds were obtained as tri-trifluoroacetates.

1-(3-Aminopropyl)-3-[3-(1*H*-imidazol-4-yl)propyl]guanidine (**115**)

The title compound was prepared from **93** (420 mg, 0.63 mmol), TFA (4 mL) and DCM (16 mL) according to the general procedure,

yielding a yellow oil (300 mg, 84%): RP-HPLC: 100%, (*t*_R = 5.94, *k* = 1.31). ¹H NMR (300 MHz, CD₃OD, tri-trifluoroacetate) δ 8.81 (d, *J* = 1.3 Hz, 1H), 7.35 (s, 1H), 3.30–3.23 (m, 4H), 3.01 (t, *J* = 7.4 Hz, 2H), 2.81 (t, *J* = 7.3 Hz, 2H), 1.96 (m, 4H). ¹³C NMR (75 MHz, CD₃OD, tri-trifluoroacetate) δ 157.66, 134.92, 134.54, 116.99, 41.68, 39.61, 38.13, 28.75, 28.02, 22.55. HRMS (ESI-MS): *m/z* [M + H⁺] calculated for C₁₀H₂₁N₆⁺: 225.1822, found 225.1822; C₁₀H₂₀N₆ x 3 TFA. (566.38).

Synthesis of the SK&F 91486 analogues 141–145

N-[3-(1-Trityl-1*H*-imidazol-4-yl)propyl]thiocarbamoyl benzamide (**137**)

Compound **137** was prepared according to the general procedure described in 4.2.5. using **5** (4.80 g, 13.06 mmol) and **28** (1.76 mL, 13.06 mmol) in 100 mL DCM. After column chromatography (EtOAc/PE 1/2 – 1/1 v/v) the product was obtained as a yellow solid (4.60 g, 66%): *R*_f = 0.55 (EtOAc/Hex 1:1); mp 139.4 °C. ¹H NMR (300 MHz, CDCl₃) δ 10.76 (bs, 1H), 9.09 (bs, 1H), 7.85–7.74 (m, 2H), 7.63–7.54 (m, 1H), 7.52–7.42 (m, 2H), 7.37 (d, *J* = 1.3 Hz, 1H), 7.39–7.25 (m, 9H), 7.20–7.05 (m, 6H), 6.60 (s, 1H), 3.72 (q, *J* = 6.9 Hz, 2H), 2.66 (t, *J* = 7.3 Hz, 2H), 2.05 (p, *J* = 7.3 Hz, 2H). ¹³C NMR (75 MHz, CDCl₃) δ 179.69, 166.76, 142.53, 140.22, 138.62, 133.46, 131.89, 129.80, 129.08, 128.05, 127.99, 127.49, 118.26, 75.14, 45.35, 27.72, 25.73. HRMS (ESI-MS): *m/z* [M + H⁺] calculated for C₃₃H₃₁N₄OS⁺: 531.2213, found 531.2218; C₃₃H₃₀N₄OS (530.69).

1-[3-(1-Trityl-1*H*-imidazol-4-yl)propyl]thiourea (**140**)

Compound **140** was prepared according to the general procedure described in 4.2.6. using **137** (1.50 g, 2.83 mmol) and K₂CO₃ (781 mg, 5.65 mmol) in 30 mL MeOH/H₂O (7/3 v/v). The product was obtained as a beige solid (920 mg, 76%): *R*_f = 0.20 (DCM/MeOH 95:5); mp 196.1 °C. ¹H NMR (400 MHz, CD₃OD) δ 7.45–7.28 (m, 10H), 7.22–7.08 (m, 6H), 6.71 (s, 1H), 3.48 + 3.13 (2 bs, 1.2H + 0.8H, (thione-thiol tautomerism)), 2.56 (t, *J* = 7.3 Hz, 2H), 1.84 (p, *J* = 7.3 Hz, 2H). ¹³C NMR (101 MHz, CD₃OD) δ 179.77, 143.76, 141.40, 139.35, 130.88, 129.28, 129.24, 119.92, 76.77, 45.09, 29.93, 26.03. HRMS (ESI-MS): *m/z* [M + H⁺] calculated for C₂₆H₂₇N₄S⁺: 427.1951, found 427.1955; C₂₆H₂₆N₄S (426.58).

N-[3-(1*H*-imidazol-4-yl)propyl]thiocarbamoyl benzamide (**141**)

The title compound was prepared from **137** (1.0 g, 1.88 mmol), TFA (4 mL) and DCM (16 mL) according to the general procedure (cf. 4.2.11). The crude product was purified by column chromatography (DCM/MeOH/7 M NH₃ in MeOH 95/3/2 v/v/v) yielding **141** as free base and yellow solid (350 mg, 64%): *R*_f = 0.12 (DCM/MeOH 95:5); mp 139.8 °C. ¹H NMR (300 MHz, CD₃OD) δ 8.01–7.84 (m, 2H), 7.71–7.62 (m, 1H), 7.61 (s, 1H), 7.57–7.46 (m, 2H), 6.88 (s, 1H), 3.72 (t, *J* = 7.0 Hz, 2H), 2.70 (t, *J* = 7.5 Hz, 2H), 2.04 (p, *J* = 7.3 Hz, 2H). ¹³C NMR (75 MHz, CD₃OD) δ 182.06, 169.56, 137.51, 135.97, 134.24, 133.95, 129.88, 129.19, 117.78, 45.70, 29.01, 25.07. HRMS (ESI-MS): *m/z* [M + H⁺] calculated for C₁₄H₁₇N₄OS⁺: 289.1118, found 289.1120; C₁₄H₁₆N₄OS (288.37); Anal. calculated for C₁₄H₁₆N₄OS: C 58.31, H 5.59, N 19.43, found: C 58.32, H 5.66, N 19.16.

N-[3-(1*H*-imidazol-4-yl)propyl]-*S*-methylisothiurea (**143**)

To an ice-cold suspension of **140** (500 mg, 1.17 mmol) in EtOH (20 mL) an aqueous solution of HI (66%, 5 mL) was added dropwise. The resulted yellow precipitate (**142** x HI) was filtrated and washed with Et₂O. Subsequently, **142** x HI was dissolved in MeOH (5 mL), treated with methyl iodide (0.08 mL, 1.29 mmol) and refluxed for

1 h. After evaporation the title compound was obtained by recrystallization in isopropanol/Et₂O to give **143** × 2 HI as a yellow-brown solid (300 mg, 56%): *R*_f = 0.10 (DCM/MeOH/NH₃ 90:10:0.1); mp 104.9 °C (2 HI). ¹H NMR (300 MHz, CD₃OD, di-hydrogen iodide) δ 8.85 (d, *J* = 1.4 Hz, 1H), 7.43 (d, *J* = 1.4 Hz, 1H), 3.46 (t, *J* = 7.2 Hz, 2H), 2.84 (t, *J* = 7.7 Hz, 2H), 2.66 (s, 3H), 2.02 (p, *J* = 7.5 Hz, 2H). ¹³C NMR (75 MHz, CD₃OD, di-hydrogen iodide) δ 170.42, 135.07, 134.21, 117.59, 44.74, 27.96, 22.99, 15.40. HRMS (ESI-MS): *m/z* [M + H⁺] calculated for C₈H₁₃N₄S⁺: 199.1012, found 199.1012; C₈H₁₄N₄S × 2 HI (454.11); Anal. calculated for C₇H₁₂N₄S × 2 HI: C 21.16, H 3.55, N 12.34, found: C 21.23, H 3.87, N 12.08.

1-[3-(1H-Imidazol-4-yl)propyl]urea (**145**)

A suspension of **144** (120 mg, 0.44 mmol) in an aqueous solution of NaOH (1 M, 10 mL) was refluxed for 1 h. After cooling of the clear solution (!) a colorless solid precipitated. After filtration the title compound was washed with Et₂O to give **145** (50 mg, 67%): *R*_f = 0.12 (DCM/MeOH/NH₃ 90:10); mp 128.0 °C. ¹H NMR (400 MHz, DMSO-*d*₆) δ 7.61 (s, 1H), 6.77 (s, 1H), 6.00 (t, *J* = 5.9 Hz, 1H), 5.40 (s, 2H), 2.97 (q, *J* = 6.5 Hz, 2H), 2.47 (t, *J* = 7.8 Hz, 2H), 1.63 (p, *J* = 7.2 Hz, 2H). ¹³C NMR (101 MHz, DMSO-*d*₆) δ 159.25, 135.91, 134.79, 117.58, 39.19, 30.38, 23.94. HRMS (ESI-MS): *m/z* [M + H⁺] calculated for C₇H₁₃N₄O⁺: 169.1084, found 169.1088; C₇H₁₂N₄O (168.20); Anal. calculated for C₇H₁₂N₄O₂ × 0.24 DMSO (sample was a recovery of a NMR sample solved in DMSO): C 48.06, H 7.25, N 29.97, found: C 48.00, H 7.11, N 30.11.

Pharmacological Methods and Materials

Materials

Histamine dihydrochloride was acquired from Alfa Aesar GmbH & Co. KG (Karlsruhe, Germany). [³H]mepyramine (specific activity: 20.0 Ci/mmol), [³H]tiotidine (specific activity: 78.4 Ci/mmol), [³H]N^ε-methylhistamine (specific activity: 85.3 Ci/mmol) and [³H]histamine (specific activity: 25.0 Ci/mmol) were purchased from Hartmann analytic (Braunschweig, Germany). GTPγS was from Roche (Mannheim, Germany), and [³⁵S]GTPγS was bought from PerkinElmer Life Science (Boston, USA) or Hartmann Analytic (Braunschweig, Germany). [³H]JUR-DE257 was synthesized in our laboratories. All stock solutions were dissolved in millipore water or in a mixture of Millipore water/DMSO. In all assays, the final DMSO content included less than 0.5%.

Methods

All the pharmacological methods used in this study (Membrane Preparation of Sf9 Cells, Radioligand Binding Assay, [³⁵S]GTPγS Binding Assay, Histamine H₁ Receptor Assay on Isolated Guinea Pig Ileum, Histamine H₂ Receptor Assay on the Isolated Guinea Pig Right Atrium) were already described in the literature.^[34]

Computational Methods

Homology modelling of both hH₄R and hH₃R, based on the crystal structure of the inactive state hH₁R (PDB ID: 3RZE)^[67] is described by Pockes et al.^[40] Protein and ligand preparation as well as the assignment of protonation states (Schrödinger LLC, Portland, OR USA) were essentially performed as described in Pegoli et al.^[68] Disulfide bonds were maintained between C87^{3.25} and C164^{ECL2} (hH₄R) and C107^{3.25} and C188^{ECL2} (hH₃R). While the isothiouraea moiety of **143** was protonated, the imidazole ring was considered in both deprotonated (τ-H or π-H) and protonated (τ-H and π-H)

form, resulting in a net charge of +1 or +2, respectively. „Flexible“ docking of **143** to both the hH₄R and hH₃R was performed using the induced fit docking module (Schrödinger LLC). **143** was docked within a box of 46 × 46 × 46 Å³ around the center of mass of the residues D94^{3.32}, E182^{5.46}, Q347^{7.42} (hH₄R) or D114^{3.32}, E206^{5.46} and L401^{7.42} (hH₃R). Redocking was performed in the extended precision mode. Furthermore, the resulting poses were scored using MM-GBSA (Schrödinger LLC). Among the reasonable ligand binding poses, the pose corresponding to the lowest MM-GBSA value, was selected as the most probable pose. Figures showing molecular structures of the hH₄R or hH₃R in complex with **143** were generated with PyMOL Molecular Graphics system, version 2.2.0 (Schrödinger LLC), and the corresponding ligand interaction diagrams were prepared with Maestro (Schrödinger LLC).

Acknowledgements

The authors thank Christine Braun, Kerstin Röhl and Maria Beer-Krön for expert technical assistance, as well as the Leibnitz Rechenzentrum (LRZ) in Munich for providing software (Schrödinger Suite) and computing resources.

Conflict of Interest

The authors declare no conflict of interest.

Keywords: histamine H₁₋₄ receptor · ligand design · receptor subtype selectivity · organ pharmacology · computational chemistry

- [1] A. Windaus, W. Vogt, *Ber. Dtsch. Chem. Ges.* **1907**, *40*, 3685–3691.
- [2] A. S. F. Ash, H. O. Schild, *Br. J. Pharmacol. Chemother.* **1966**, *27*, 427–439.
- [3] J. W. Black, W. A. M. Duncan, C. J. Durant, C. R. Ganellin, E. M. Parsons, *Nature* **1972**, *236*, 385–390.
- [4] J.-M. Arrang, M. Garbarg, J.-C. Schwartz, *Nature* **1983**, *302*, 832–837.
- [5] T. Oda, N. Morikawa, Y. Saito, Y. Masuho, S. Matsumoto, *J. Biol. Chem.* **2000**, *275*, 36781–36786.
- [6] M. C. Lagerström, H. B. Schiöth, *Nat. Rev. Drug Discovery* **2008**, *7*, 339–357.
- [7] S. J. Hill, *Pharmacol. Rev.* **1990**, *42*, 45–83.
- [8] R. Leurs, M. J. Smit, H. Timmerman, *Pharmacol. Ther.* **1995**, *66*, 413–463.
- [9] S. J. Hill, C. R. Ganellin, H. Timmerman, J. C. Schwartz, N. P. Shankley, J. M. Young, W. Schunack, R. Levi, H. L. Haas, *Pharmacol. Rev.* **1997**, *49*, 253–278.
- [10] A. H. Soll, A. Wollin, *Am. J. Physiol. Gastrointest. Liver Physiol.* **1979**, *237*, G444–G450.
- [11] C. L. Johnson, H. Weinstein, J. P. Green, *Mol. Pharmacol.* **1979**, *16*, 417–428.
- [12] J. Fischer, C. R. Ganellin, A. Ganesan, J. Proudfoot, *Analogue-Based Drug Discovery*, Wiley-VCH, **2010**.
- [13] H. Van Der Goot, H. Timmerman, *Eur. J. Med. Chem.* **2000**, *35*, 5–20.
- [14] A. Rouleau, X. Ligneau, J. Tardivel-Lacombe, S. Morisset, F. Gbahou, J.-C. Schwartz, J.-M. Arrang, *Br. J. Pharmacol.* **2002**, *135*, 383–392.
- [15] R. Leurs, P. L. Chazot, F. C. Shenton, H. D. Lim, I. J. De Esch, *Br. J. Pharmacol.* **2009**, *157*, 14–23.
- [16] K. L. Morse, J. Behan, T. M. Laz, R. E. West, S. A. Greenfeder, J. C. Anthes, S. Umland, Y. Wan, R. W. Hipkin, W. Gonsiorek, *J. Pharmacol. Exp. Ther.* **2001**, *296*, 1058–1066.
- [17] T. W. Lovenberg, B. L. Roland, S. J. Wilson, X. Jiang, J. Pyati, A. Huvar, M. R. Jackson, M. G. Erlander, *Mol. Pharmacol.* **1999**, *55*, 1101–1107.
- [18] Y. Zhu, D. Michalovich, H.-L. Wu, K. B. Tan, G. M. Dytko, I. J. Mannan, R. Boyce, J. Alston, L. A. Tierney, X. Li, *Mol. Pharmacol.* **2001**, *59*, 434–441.
- [19] C. Liu, X.-J. Ma, X. Jiang, S. J. Wilson, C. L. Hofstra, J. Blevitt, J. Pyati, X. Li, W. Chai, N. Carruthers, *Mol. Pharmacol.* **2001**, *59*, 420–426.

- [20] C. L. Hofstra, P. J. Desai, R. L. Thurmond, W.-P. Fung-Leung, *J. Pharmacol. Exp. Ther.* **2003**, *305*, 1212–1221.
- [21] M. J. Gemkow, A. J. Davenport, S. Harich, B. A. Ellenbroek, A. Cesura, D. Hallett, *Drug Discovery Today* **2009**, *14*, 509–515.
- [22] B. Sadek, N. Khan, F. H. Darras, S. Pockes, M. Decker, *Physiol. Behav.* **2016**, *165*, 383–391.
- [23] B. Sadek, A. Saad, A. Sadeq, F. Jalal, H. Stark, *Behav. Brain Res.* **2016**, *312*, 415–430.
- [24] M. Rapanelli, *Prog. Neuro-Psychopharmacol. Biol. Psychiatry* **2017**, *73*, 36–40.
- [25] M. Rapanelli, L. Frick, V. Pogorelov, H. Ohtsu, H. Bito, C. Pittenger, *Transl. Psychiatry* **2017**, *7*, e1013–e1013.
- [26] P. J. Dunford, N. O'Donnell, J. P. Riley, K. N. Williams, L. Karlsson, R. L. Thurmond, *J. Immunol.* **2006**, *176*, 7062–7070.
- [27] R. L. Thurmond, E. W. Gelfand, P. J. Dunford, *Nat. Rev. Drug Discovery* **2008**, *7*, 41–53.
- [28] R. Leurs, H. F. Vischer, M. Wijnmans, I. J. de Esch, *Trends Pharmacol. Sci.* **2011**, *32*, 250–257.
- [29] J. A. Jablonowski, C. A. Grice, W. Chai, C. A. Dvorak, J. D. Venable, A. K. Kwok, K. S. Ly, J. Wei, S. M. Baker, P. J. Desai, *J. Med. Chem.* **2003**, *46*, 3957–3960.
- [30] E. Zampeli, E. Tiligada, *Br. J. Pharmacol.* **2009**, *157*, 24–33.
- [31] A. M. Staub, D. Bovet, *Compt. Rend. Soc. de biol* **1937**, *125*, 818.
- [32] B. N. Halpern, *Arch. Int. Pharmacodyn. Ther.* **1942**, *68*, 339–343.
- [33] P. B. Marshall, *Br. J. Pharmacol.* **1955**, *10*, 270–278.
- [34] G. J. Durant, W. A. M. Duncan, C. R. Ganellin, M. E. Parsons, R. C. Blakemore, A. C. Rasmussen, *Nature* **1978**, *276*, 403–405.
- [35] G. J. Durant, C. R. Ganellin, D. W. Hills, P. D. Miles, M. E. Parsons, E. S. Pepper, G. R. White, *J. Med. Chem.* **1985**, *28*, 1414–1422.
- [36] A. Buschauer, *J. Med. Chem.* **1989**, *32*, 1963–1930.
- [37] M. E. Parsons, R. C. Blakemore, G. J. Durant, C. R. Ganellin, A. C. Rasmussen, *Inflamm. Res.* **1975**, *5*, 464–464.
- [38] H. D. Lim, R. M. van Rijn, P. Ling, R. A. Bakker, R. L. Thurmond, R. Leurs, *J. Pharmacol. Exp. Ther.* **2005**, *314*, 1310–1321.
- [39] J. C. Eriks, H. van der Goot, G. J. Sterk, H. Timmerman, *J. Med. Chem.* **1992**, *35*, 3239–3246.
- [40] S. Pockes, D. Wifling, M. Keller, A. Buschauer, S. Elz, *ACS Omega* **2018**, *3*, 2865–2882.
- [41] A. Kraus, P. Ghorai, T. Birnkammer, D. Schnell, S. Elz, R. Seifert, S. Dove, G. Bernhardt, A. Buschauer, *ChemMedChem* **2009**, *4*, 232–240.
- [42] T. Birnkammer, A. Spickenreither, I. Brunskole, M. Lopuch, N. Kagermeier, G. Bernhardt, S. Dove, R. Seifert, S. Elz, A. Buschauer, *J. Med. Chem.* **2012**, *55*, 1147–1160.
- [43] N. Kagermeier, K. Werner, M. Keller, P. Baumeister, G. Bernhardt, R. Seifert, A. Buschauer, *Bioorg. Med. Chem.* **2015**, *23*, 3957–3969.
- [44] R. Yang, J. A. Hey, R. Aslanian, C. A. Rizzo, *Pharmacology* **2002**, *66*, 128–135.
- [45] P. Igel, R. Geyer, A. Strasser, S. Dove, R. Seifert, A. Buschauer, *J. Med. Chem.* **2009**, *52*, 6297–6313.
- [46] P. Igel, E. Schneider, D. Schnell, S. Elz, R. Seifert, A. Buschauer, *J. Med. Chem.* **2009**, *52*, 2623–2627.
- [47] P. Ghorai, A. Kraus, M. Keller, C. Götte, P. Igel, E. Schneider, D. Schnell, G. Bernhardt, S. Dove, M. Zabel, *J. Med. Chem.* **2008**, *51*, 7193–7204.
- [48] O. Mitsunobu, M. Yamada, T. Mukaiyama, *Bull. Chem. Soc. Jpn.* **1967**, *40*, 935–939.
- [49] C. Dardonville, C. Fernandez-Fernandez, S.-L. Gibbons, G. J. Ryan, N. Jagerovic, A. M. Gabilondo, J. J. Meana, L. F. Callado, *Bioorg. Med. Chem.* **2006**, *14*, 6570–6580.
- [50] S. M. Hickey, T. D. Ashton, S. K. Khosa, F. M. Pfeffer, *Synlett* **2012**, *23*, 1779–1782.
- [51] N. Pluym, A. Brennauer, M. Keller, R. Ziemek, N. Pop, G. Bernhardt, A. Buschauer, *ChemMedChem* **2011**, *6*, 1727–1738.
- [52] A. Buschauer, *J. Med. Chem.* **1989**, *32*, 1963–1970.
- [53] J. W. Black, G. J. Durant, J. C. Emmett, C. R. Ganellin, *Thioureas*, **1973**, GB1305548A.
- [54] J. W. Black, G. J. Durant, J. C. Emmett, C. R. Ganellin, *Isothioureas*, **1973**, GB1305547A.
- [55] D. B. Frennsson, D. R. Langley, M. G. Saulnier, D. M. Vyas, *Methods for Preparing Macrocycles and Macrocyclic Stabilized Peptides*, **2012**, WO2012051405A1.
- [56] W. Carling, K. Moore, *Imidazolone and Oxazolone Derivatives as Dopamine Antagonists*, European Patent Office, Rijswijk, **1995**, WO 95/07904.
- [57] K. S. Kim, L. Qian, *Int. J. Rapid Publ. Prelim.* **1993**, *34*, 7677–7680.
- [58] R. W. Brimblecombe, W. A. M. Duncan, G. J. Durant, J. C. Emmett, C. R. Ganellin, M. E. Parsons, *J. Int. Med. Res.* **1975**, *3*, 86–92.
- [59] R. W. Brimblecombe, W. A. M. Duncan, G. J. Durant, C. R. Ganellin, M. E. Parsons, J. W. Black, *Br. J. Pharmacol.* **1975**, *53*, 435–436.
- [60] L. B. Hough, *Mol. Pharmacol.* **2001**, *59*, 415–419.
- [61] C. Robin Ganellin, J. C. Schwartz, H. Stark, *Successful Drug Discovery* **2018**, *3*, 359–381.
- [62] J. B. Baell, G. A. Holloway, *J. Med. Chem.* **2010**, *53*, 2719–2740.
- [63] C. Aldrich, C. Bertozzi, G. I. Georg, L. Kiessling, C. Lindsley, D. Liotta, K. M. Merz, A. Schepartz, S. Wang, *ACS Cent. Sci.* **2017**, *3*, 143–147.
- [64] S. M. Devine, M. D. Mulcair, C. O. Debono, E. W. W. Leung, J. W. M. Nissink, S. S. Lim, I. R. Chandrashekar, M. Vazirani, B. Mohanty, J. S. Simpson, J. B. Baell, P. J. Scammells, R. S. Norton, M. J. Scanlon, *J. Med. Chem.* **2015**, *58*, 1205–1214.
- [65] M. Nettekoven, W. Guba, W. Neidhart, P. Mattei, P. Pflieger, O. Roche, S. Taylor, *Bioorg. Med. Chem. Lett.* **2005**, *15*, 3446–3449.
- [66] V. S. Aulakh, A. Casarez, X. Lin, M. Lindvall, G. McEnroe, H. E. Moser, F. Reck, M. Tjandra, R. L. Simmons, A. Yifru, *Preparation of Monobactam Organic Compounds for the Treatment of Bacterial Infections*, **2015**, US 20150266867A1.
- [67] T. Shimamura, M. Shiroishi, S. Weyand, H. Tsujimoto, G. Winter, V. Katritch, R. Abagyan, V. Cherezov, W. Liu, G. W. Han, *Nature*, **2011**, *475*, 65–70.
- [68] A. Pegoli, X. She, D. Wifling, H. Hübner, G. Bernhardt, P. Gmeiner, M. Keller, *J. Med. Chem.* **2017**, *60*, 3314–3334.

 Manuscript received: January 10, 2019

Revised manuscript received: February 8, 2019